Journal of Optoelectronics and Advanced Materials Vol 1, No. 4, December 1999, p. 33-41

OPTICAL PROPERTIES OF GERMANIUM-GALLIUM-SELENIDE GLASSES DOPED BY SAMARIUM

P. Němec, J. Oswald[a], M. Frumar, B. Frumarová[b]

Department of General and of Inorganic Chemistry, University of Pardubice, 53210 Pardubice, Czech Republic,
[a]Institute of Physics of Czech Acad. Sci., Prague, Czech Republic,
[b]Joint Laboratory of Solid State Chemistry of Czech Acad. of Sci. and University of Pardubice, 53210 Pardubice, Czech Republic

Samarium-doped $Ge_{30}Ga_5Se_{65}$ glasses were synthesized and investigated. The experimental oscillator strengths of five f-f electron transitions and Judd-Ofelt intensity parameters of Sm^{3+} ions were determined from the transmission spectra at room temperature. In the emission spectra of samarium-doped $Ge_{30}Ga_5Se_{65}$ glasses, three luminescence bands near 1080, 1240 and 1490 nm were observed and their properties discussed. The problem of distortion of emission spectra as a consequence of light absorption by Sm^{3+} ions is also discussed. On the basis of the Judd-Ofelt theory, spontaneous emission probabilities and branching ratios of radiative electron transitions of Sm^{3+} ions were calculated.

(Received November 22, 1999; accepted November 30, 1999)

Keywords: Selenide glasses, Samarium, Optical properties, Luminescence

1. Introduction

Optical properties of rare-earth (RE) ions incorporated in glassy matrices have been, recently, extensively studied (see, e.g. [1,2]). This fact is due to possible applications of these materials for solid state lasers, fibre amplifiers, up-conversion devices and other optoelectronics components in visible, near- and mid-infrared spectral regions. In such devices, radiative electron transitions between discrete energy levels of RE^{3+} ions introduced into glassy host can be applied. Chalcogenide glasses are of large interest as hosts for doping with RE elements or compounds, at least due to two main reasons. Firstly, low phonon energy of such materials, which results in low non-radiative decay rates of RE energy levels [3] is very attractive. Secondly, the long-wavelength absorption edge of chalcogenide glasses is shifted towards longer wavelengths [4,5] when compared with oxide and halide glasses. This gives them good transparency in the infrared region of the spectrum. Chalcogenide glasses exhibit high indices of refraction, which are important for some applications. High value of the refractive index leads to high spontaneous emission probability and, consequently, to large emission cross-sections of radiative electron transitions between energy levels of RE ions. Low phonon energy and high index of refraction facilitate high quantum efficiencies of the optical transitions originating from the energy levels which are close to the next lower-lying levels (small energy gap). It is, therefore, possible to observe radiative electron transitions of RE^{3+} ions, which are in conventional oxide or fluoride glasses doped by RE^{3+} ions usually quenched [3,4]. A disadvantage of some chalcogenide glasses is their lower transparency in visible (VIS) or near-infrared (NIR) spectral regions due to their smaller optical gap, E_g^{opt}. Lower transparency of such materials in these spectral regions excludes the possibility of application of UV or VIS luminescence of RE^{3+} ions, because of fundamental absorption of glassy host.

Most papers devoted to the research of RE-doped non-oxide glasses have been concerned with optical properties of Er^{3+}-, Nd^{3+}-, or Pr^{3+}-doped hosts (see, e.g. [1-3, 6,7] and papers cited

therein). The glasses doped by samarium have received a relatively less attention, because of smaller emission efficiencies of radiative electron transitions between energy levels of Sm^{3+} ions and because of reported valence instability [6-9]. The papers on Sm^{3+}-doped glasses mostly were concerned with the luminescence in the visible region of the spectrum [6-9]. The emission spectra in this region can be related to the electron transitions from $^4G_{5/2}$ level of Sm^{3+} ions to the ^6H_J manifold [6-8]. A laser action of Sm^{3+}-doped silica fibre at 650 nm was also reported [9].

In this paper, the solubility of samarium in a germanium-gallium-selenium glass ($Ge_{30}Ga_5Se_{65}$) was determined and results of analysis of some optical properties of this glass are presented. On the basis of Judd-Ofelt analysis, are discussed the radiative properties of Sm^{3+} ions in the near infrared spectral region.

2. Experimental

The glasses were synthesized from high purity elements (Ge, Ga and Se all of 5N-purity) and from Sm (99.9%) in sealed and evacuated silica ampoules in a rocking furnace. The maximum temperature and the period of the synthesis were 960°C and 20 hours, respectively. After the synthesis, the ampoules with the melt were stabilized at 750°C for 4h, water quenched and immediately inserted in an annealing furnace. The samples were annealed at 320°C (~30°C below the glass transition temperature, T_g) for 3 hours and after annealing they were slowly cooled (3°C/min) to the room temperature.

The transmission spectra of cut and polished plan-parallel plates of prepared glasses were measured using spectrophotometer JASCO V-570 (500 - 2500 nm) and FT spectrophotometer BIO-RAD FTS 175C (2500 - 25000 nm).

The room temperature Raman spectra were recorded by FT-IR spectrophotometer IFS 55 provided with Raman FRA-106 accessory (Bruker). A backscattering method with the YAG:Nd laser (1064 nm) as the excitation light was used.

The room temperature luminescence spectra were measured on polished bulk samples in the spectral region between 1050 and 1600 nm using 180° geometry and back-scattering method. For the luminescence excitation light sources at 980 nm (laser diode) and 1064 nm (Nd-doped YAG laser) were used. For detection of emission spectra in NIR spectral region a liquid-nitrogen cooled Ge detector was used.

The refractive index of polished bulk samples was determined using the ellipsometric method in the spectral region 300-1200 nm.

3. Results

Pure and doped $Ge_{30}Ga_5Se_{65}$ glasses were investigated. It was found that up to 1 mol% of Sm can be introduced in $Ge_{30}Ga_5Se_{65}$ glass without any observable crystallization (by optical and electron microscopy, X-ray diffraction). The glasses of the system $(Ge_{30}Ga_5Se_{65})_{100-x}(Sm_2Se_3)_x$, (x = 0, 0.01, 0.05, 0.1, 0.2, 0.3, 0.5) are black. In comparison with analogous sulfide glasses, the position of the short-wavelength absorption edge is shifted to the near infrared spectral region (670-870 nm, Fig. 1). Because of limited transparency of the studied glasses in visible spectral region, only absorption bands connected with optical transitions in Sm^{3+} ions in the infrared region were observed in room-temperature transmission spectra of studied glasses (Fig. 1).

The long-wavelength absorption edge of the glasses was found near 700 cm^{-1} (> 14 μm) and its position can be assigned to the multiphonon Ge-Se vibrations [10].

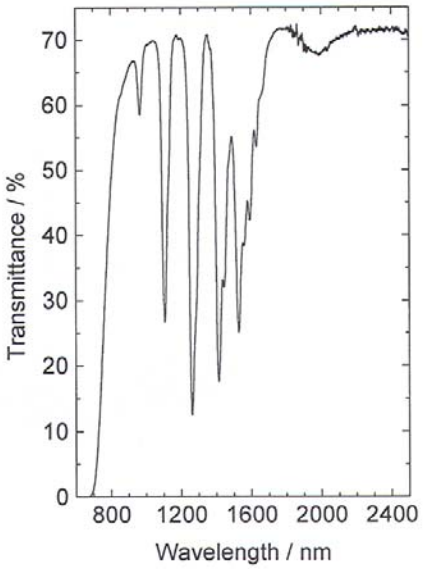

Fig. 1 The room temperature transmission spectra of the $(Ge_{30}Ga_5Se_{65})_{99.5}(Sm_2Se_3)_{0.5}$ glass.

The experimental oscillator strengths for the infrared absorption bands were determined after [11]. The best-resolved absorption bands in the near infrared spectral region near 970, 1110, 1260, 1410 and 1530 nm were included in these calculations. The absorption bands with maxima near 1410 and 1530 nm overlap (Fig. 1). For the determination of individual experimental strengths of oscillator, the overlapped absorption bands were separated by deconvolution procedure. On the basis of Judd-Ofelt theory [12,13], three intensity parameters, Ω_t, where t = 2, 4, 6, were evaluated using experimentally found oscillator strengths (Table 1). From the Judd-Ofelt intensity parameters Ω_t, the spontaneous transition probabilities and branching ratios among energy levels of Sm^{3+} ions were calculated.

Table 1
Observed (f_{exp}) and calculated (f_{cal}) oscillator strengths of f-f electron transitions of Sm^{3+} ions in $Ge_{30}Ga_5Se_{65}$ glass

Transition from $^6H_{5/2}$ to	Wavelength (nm)	f_{exp} (10^{-8})	f_{cal} (10^{-8})
$^6F_{1/2}$, $^6H_{15/2}$, $^6F_{3/2}$	1528	1518	1519
$^6F_{5/2}$	1414	1597	1586
$^6F_{7/2}$	1262	1961	1985
$^6F_{9/2}$	1108	1200	1175
$^6F_{11/2}$	966	193	187

The room temperature luminescence spectra of the investigated glasses doped with samarium are given in Figs. 2-3. Three luminescence bands near 1080, 1240 and 1490 nm were observed, when excited by 980 nm light (Fig. 2).

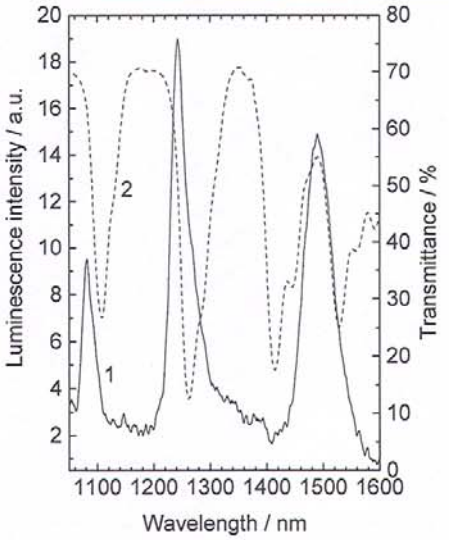

Fig. 2 The room temperature luminescence spectra of the $(Ge_{30}Ga_5Se_{65})_{99.9}(Sm_2Se_3)_{0.1}$ glass, excited by 980 nm light (1) and the transmittance spectrum (2).

All three luminescence bands can be assigned to the electron transitions between the discrete energy levels of Sm^{3+} ions, as will be discussed later. The emission spectra were also excited by longer excitation wavelength (1064 nm, Nd:YAG laser) using backscattering method (Fig. 3). The luminescence spectrum was different in this case. The luminescence bands were strongly distorted, probably due to absorption in Sm^{3+} ions (Fig. 3).

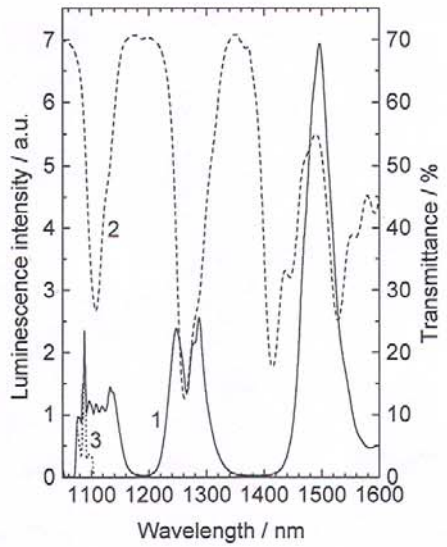

Fig. 3 The room temperature luminescence spectra of the $(Ge_{30}Ga_5Se_{65})_{99.9}(Sm_2Se_3)_{0.1}$ glass, excited by 1064 nm light (1). The absorption curve of Sm^{3+} doped glass (2) and Raman scattering (3) are also given.

From the Raman spectrum of pure $Ge_{30}Ga_5Se_{65}$ glass, the maximum phonon energy (~ 320 cm^{-1}) was determined. Detailed analysis of the Raman spectra and of the structure of Ge-Ga-Se glasses is given in Ref. [10].

4. Discussion

In the room-temperature transmission spectrum of $(Ge_{30}Ga_5Se_{65})_{99.5}(Sm_2Se_3)_{0.5}$ glass, several sharp absorption bands with maxima at around 970, 1110, 1260, 1410, 1530 and 1990 nm can be observed (Fig. 1). Further absorption bands in mid-infrared spectral region are centred near 2700, 4500 and 9600 nm. Analogously with [6-8], these absorption bands can be assigned to the electron transitions between $^6H_{5/2}$ ground level and higher energy levels of manifolds ^6F_J (J = 11/2, 9/2, 7/2, 5/2, 3/2, 1/2) and ^6H_J (J = 15/2, 13/2, 11/2, 9/2, 7/2) of Sm^{3+} ions (see also Fig. 4). The absorption bands of Sm^{3+} ions in the visible spectral region are hidden because of fundamental absorption of the glassy matrix. It should be noted that only absorption bands which can be assigned to the electron transitions of Sm^{3+} ions were found in high transparency region of studied glasses. The areas of absorption bands of Sm^{3+} ions grow with increasing content of samarium nearly linearly (Fig. 5). The Sm^{3+} ions apparently do not change their valency and their optical activity when their concentration in the glassy matrix increases.

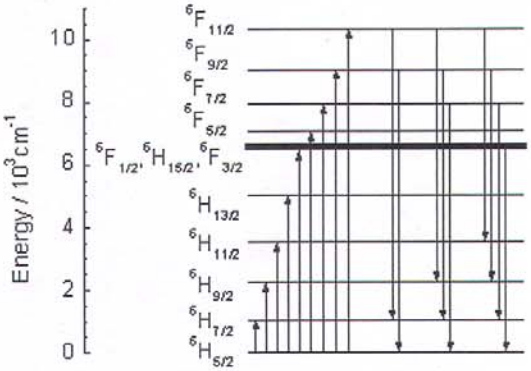

Fig. 4 Energy scheme of electron transitions in Sm^{3+} ions in Ge-Ga-Se glasses.

From the room temperature transmission spectra of the $(Ge_{30}Ga_5Se_{65})_{99.5}(Sm_2Se_3)_{0.5}$ glass, the experimental oscillator strengths of electric dipole transitions of Sm^{3+} ions were calculated. To our knowledge, the found oscillator strengths in the investigated Ge-Ga-Se glasses (Table 1) are the highest among the known Sm^{3+}-doped glasses [6,8].

Judd-Ofelt intensity parameters were evaluated by the least-squares fitting method analogously as described in [12,13] using Eq. (1) and the measured oscillator strengths (Table 1)

$$f_{cal}\left((S,L)J,(S',L')J'\right)=\frac{8\pi^2 m\upsilon}{3h(2J+1)}\left[\frac{\left(n^2+2\right)^2}{9n}\sum_{t=2,4,6}\Omega_t\left|\left\langle (S,L)J\left\|U^{(t)}\right\|(S',L')J'\right\rangle\right|^2\right], \qquad (1)$$

where f_{cal} are the calculated oscillator strengths, h is Planck's constant, m is electron mass, υ is mean wavenumber of the absorption band, J is the ground-state total angular momentum of Sm^{3+} (J=5/2), n is the refractive index of the material, Ω_t are the Judd-Ofelt phenomenological intensity parameters and the $\left\langle (S,L)J\left\|U^{(t)}\right\|(S',L')J'\right\rangle$ are the reduced matrix elements of the tensor operator, $U^{(t)}$ of rank t. The reduced matrix elements, $U^{(t)}$, are only slightly sensitive to the composition of the host and, therefore, the $U^{(t)}$ elements calculated by Carnall et al. [14] for Sm^{3+} in LaF_3 were used. Accuracy of the least-squares fitting method was evaluated by the root-mean-square (rms) deviation using the measured oscillator strengths, which is defined as follows:

$$rms=\left(\frac{\sum\left(f_{\exp}-f_{cal}\right)^2}{n_{transitions}-n_{parameters}}\right)^{1/2}, \qquad (2)$$

where f_{exp} and f_{cal} are experimental and calculated oscillator strengths, respectively.

Values of the Judd-Ofelt intensity parameters obtained for Sm^{3+} ions in Ge-Ga-Se glasses were found to be $\Omega_2 = 7.423 \times 10^{-20}$ cm^2, $\Omega_4 = 14.428 \times 10^{-20}$ cm^2, $\Omega_6 = 6.428 \times 10^{-20}$ cm^2. These

values are to our knowledge the highest ones found in Sm^{3+}-doped glasses. Root-mean-square deviation, which represents the quality of the fit, is equal 2.626×10^{-7}.

From the Judd-Ofelt intensity parameters, Ω_t, important radiative properties associated with optical electron transitions between energy levels of Sm^{3+} ions can be calculated. The spontaneous transition probability A of an electric-dipole transition is determined [5,11] from the Eq. 3:

$$A[(S,L)J;(S',L')J'] = \frac{64\pi^4 e^2 n}{3h(2J+1)\bar{\lambda}^3}\left[\frac{(n^2+2)^2}{9}\right] \times \sum_{t=2,4,6} \Omega_t \left|\left\langle (S,L)J \left\| U^{(t)} \right\| (S',L')J' \right\rangle\right|^2 , \quad (3)$$

where e is the electron charge and $\bar{\lambda}$ is the average wavelength of the transition.

For optical transitions, which originate from overlapping energy levels, the effective emission rate A_{eff} was calculated from the individual spontaneous transition probabilities (assuming that the energy gap between the overlapping levels is negligible) according to the Eq. (4), which is analogous to the equation used in Ref. [15]

$$A_{eff} = \frac{g_1 A_1 + g_2 A_2 + \ldots + g_n A_n}{g_1 + g_2 + \ldots + g_n}, \quad (4)$$

where g_1 , g_2 and g_n are the degeneracy of the levels, A_1 , A_2 and A_n are the individual radiative rates.

The fluorescence branching ratio β of electron transitions from an initial manifold level $|(S,L)J\rangle$ to lower levels $|(S',L')J'\rangle$ is given by [5]

$$\beta[(S,L)J;(S',L')J'] = \frac{A[(S,L)J;(S',L')J']}{\sum_{S',L',J'} A[(S,L)J;(S',L')J']}. \quad (5)$$

The values of wavelengths, spontaneous emission probabilities and of branching ratios connected with radiative electron transitions from manifold level ^6F_J (J=11/2, 9/2, 7/2, 5/2, 3/2, 1/2) and $^6H_{15/2}$ level of Sm^{3+} ions are summarized in Table 2.

At the room temperature, three emission bands near 1080, 1240 and 1490 nm can be observed in the luminescence spectrum of Sm^{3+}-doped Ge-Ga-Se glasses when excited by 980 nm light (Fig. 2). First emission band near 1080 nm with the effective bandwidth (or full width at half maximum of intensity of luminescence (FWHM)) ~33 nm can be assigned to the radiative electron transitions between the energy levels $^6F_{11/2}$ and $^6H_{7/2}$ (Fig. 4), which have a branching ratio of 13% (Table 2). Electrons are excited by 980 nm radiation directly to $^6F_{11/2}$ energy level. After the emission of light due to radiative electron transitions $^6F_{11/2}$ - $^6H_{7/2}$, the depletion of the energy level $^6H_{7/2}$ to the ground state $^6H_{5/2}$ level runs probably by multiphonon relaxation process or by emission of light with wavelength around λ = 9.5 μm. It cannot be excluded, that the form of emission spectra is partly influenced by absorption (re-absorption) of light by Sm^{3+} ions. When the luminescence is excited by 1064 nm light, the absorption effect is probably stronger and the emission band $^6F_{11/2}$ - $^6H_{7/2}$ is heavily distorted due to strong absorption band of Sm^{3+} ions in the region. To less extent it is also distorted due to Raman scattering (Fig. 3). It can be supposed, that the electrons cannot be excited directly to the energy level $^6F_{11/2}$, because of lower energy of excitation light (1064 nm), but only with contribution of several phonons. The probability of such transitions should be lower.

The emission band near 1120 nm (Fig. 3) is also splitted (weak narrow bands). We believe that such a splitting of emission band can be explained by Stark splitting of energy levels $^6F_{11/2}$ and/or $^6H_{7/2}$. The contribution of $^6F_{9/2}$ - $^6H_{5/2}$ radiative electron transitions (Fig. 4), which have relatively large spontaneous emission probability and branching ratio, can be also assumed (Table 2). The presence of electrons on energy level $^6F_{9/2}$ may be caused by multiphonon relaxation process.

When pumped by 980 nm light, the second luminescence band in the emission spectra of samarium-doped $Ge_{30}Ga_5Se_{65}$ glasses is centered near 1240 nm and has a bandwidth of ~ 44 nm (Fig.2). This emission band is probably connected with radiative electron transitions $^6F_{11/2}$ - $^6H_{9/2}$ (Fig. 4). Depopulation of $^6H_{9/2}$ energy level can proceed again via several phonons and/or by emission of light with band maximum near 4.5 μm ($^6H_{9/2}$ - $^6H_{5/2}$).

More complex luminescence band, which is a little broader (FWHM ~65 nm), can be found in the region between 1220-1320 nm (Fig. 3) when excited by 1064 nm light. This emission band is probably distorted by strong absorption band of Sm^{3+} ions as we have mentioned above (Fig. 3). It can be also formed by overlapping of three different possible radiative electron transitions $^6F_{11/2}$ - $^6H_{9/2}$,

$^6F_{9/2}$ - $^6H_{7/2}$ and $^6F_{7/2}$ - $^6H_{5/2}$ (Fig. 4) of Sm^{3+} ions. By comparing the parameters of the described transitions (Table 2) we can advance the hypothesis that these transitions proceed simultaneously.

Table 2

Probable radiative electron transitions in Sm^{3+} ions with corresponding wavelengths (calculated from absorption spectra), spontaneous emission probabilities, $A(s^{-1})$, and branching ratios β (%).

Transition from to	λ (nm)	A (s^{-1})	β (%)
$^6F_{11/2} \rightarrow {}^6H_{5/2}$	966	407	4
$\rightarrow {}^6H_{7/2}$	1075	1405	13
$\rightarrow {}^6H_{9/2}$	1233	2504	23
$\rightarrow {}^6H_{11/2}$	1469	2958	27
$\rightarrow {}^6H_{13/2}$	1879	2335	21
$\rightarrow {}^6F_{1/2}$	2627	11	0
$\rightarrow {}^6H_{15/2}$	2627	1241	11
$\rightarrow {}^6F_{3/2}$	2627	22	0
$\rightarrow {}^6F_{5/2}$	3049	25	0
$\rightarrow {}^6F_{7/2}$	4119	15	0
$\rightarrow {}^6F_{9/2}$	7536	4	0
$^6F_{9/2} \rightarrow {}^6H_{5/2}$	1108	2284	23
$\rightarrow {}^6H_{7/2}$	1253	3073	30
$\rightarrow {}^6H_{9/2}$	1474	2419	24
$\rightarrow {}^6H_{11/2}$	1824	1421	14
$\rightarrow {}^6H_{13/2}$	2503	674	7
$\rightarrow {}^6F_{1/2}$	4032	2	0
$\rightarrow {}^6H_{15/2}$	4032	248	2
$\rightarrow {}^6F_{3/2}$	4032	9	0
$\rightarrow {}^6F_{5/2}$	5120	7	0
$\rightarrow {}^6F_{7/2}$	9083	1	0
$^6F_{7/2} \rightarrow {}^6H_{5/2}$	1262	3686	43
$\rightarrow {}^6H_{7/2}$	1454	2273	27
$\rightarrow {}^6H_{9/2}$	1760	1524	18
$\rightarrow {}^6H_{11/2}$	2283	791	9
$\rightarrow {}^6H_{13/2}$	3455	234	3
$\rightarrow {}^6F_{1/2}$	7252	2	0
$\rightarrow {}^6H_{15/2}$	7252	26	0
$\rightarrow {}^6F_{3/2}$	7252	1	0
$\rightarrow {}^6F_{5/2}$	11740	0	0
$^6F_{5/2} \rightarrow {}^6H_{5/2}$	1414	3131	46
$\rightarrow {}^6H_{7/2}$	1660	2228	33
$\rightarrow {}^6H_{9/2}$	2070	978	14
$\rightarrow {}^6H_{11/2}$	2834	418	6
$\rightarrow {}^6H_{13/2}$	4897	85	1
$\rightarrow {}^6F_{1/2}$	18980	0	0
$\rightarrow {}^6H_{15/2}$	18980	1	0
$\rightarrow {}^6F_{3/2}$	18980	0	0
$^6F_{3/2}$, $^6H_{15/2}$, $^6F_{1/2} \rightarrow {}^6H_{5/2}$	1528	700*	40*
$\rightarrow {}^6H_{7/2}$	1819	535*	30*
$\rightarrow {}^6H_{9/2}$	2324	347*	20*
$\rightarrow {}^6H_{11/2}$	3332	155*	9*
$\rightarrow {}^6H_{13/2}$	6601	30*	2*

The asterisks * is for effective value of spontaneous emission probability or effective branching ratio

The third emission band in the luminescence spectra (when excited by 980 nm light) with maximum near 1490 nm (Fig. 2) and with FWHM ~63 nm can be connected with $^6F_{11/2}$ - $^6H_{11/2}$ radiative electron transitions of Sm^{3+} ions (Fig. 4). It can be deduced from Table 2 that some other radiative transitions with close energy can play also a role, e.g.: $^6F_{9/2}$ - $^6H_{9/2}$, $^6F_{7/2}$ - $^6H_{7/2}$ and $^6F_{5/2}$ ($^6F_{3/2}$, $^6H_{15/2}$, $^6F_{1/2}$) - $^6H_{5/2}$. All above-mentioned transitions are possible if we suppose, that some non-radiative transitions play a role in depopulation of electrons from $^6F_{11/2}$ level. The exception is probably the $^6F_{5/2}$ - $^6H_{5/2}$ transition, which should be completely quenched because of very low energy gap to the next lower lying $^6F_{3/2}$ level (530 cm^{-1}). In contrast to the bands near 1080 and 1240 nm, the emission band near 1490 nm is unchanged when excited either by 1064 nm light (using back-scattering arrangement) or by 980 nm excitation light.

The luminescence spectra are relatively complex and their unambiguous assignment and explanation needs further study.

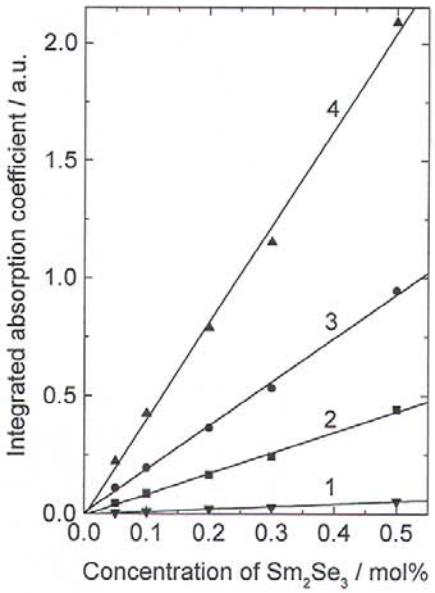

Fig. 5 Concentration dependence of areas of absorption bands assigned to electron transitions of Sm^{3+} ions. Maxima of absorption bands are around: 1-970 nm, 2-1110 nm, 3-1260 nm, 4-1410 nm.

From the concentration dependence of the luminescence intensity it is obvious, that the luminescence decreases with increasing concentration of samarium for $c \geq 0.2$ mol% of Sm^{3+}. This fact is probably caused by two factors. First factor is the well-known concentration quenching of the luminescence intensity, the second factor is the above-mentioned re-absorption of emitted light as a consequence of strong absorption bands in the near infrared spectral region.

The above discussed infrared emission bands of Sm^{3+}-doped Ge-Ga-Se glasses occur due to very low phonon energy of the glass matrix. Maximum of the phonon energy is to ~320 cm^{-1}, as determined from the Raman spectra of studied glasses. Because of this small value, the non-radiative multiphonon processes are effectively reduced. For example, the energy gap between the energy states $^6F_{11/2}$ and $^6F_{9/2}$ is ~1330 cm^{-1}. The highest phonon energy in silicate glasses is ~1100 cm^{-1} and only one or two phonons are necessary to quench radiative transitions from $^6F_{11/2}$ energy level. On the other hand, about four or five phonons are required to bridge the same energy gap, when Ge-Ga-Se glasses used as hosts for Sm^{3+} ions. Such transitions are much less probable.

5. Conclusion

We have reported results on material preparation and measurements of optical properties of samarium doped Ge-Ga-Se glasses. The phonon energies of selenide glasses are even lower than of sulfide ones. Because of low phonon energy of the glassy matrix, the studied glasses exhibit unique luminescence properties. The reduced multiphonon relaxation rate can result in higher quantum efficiency and supports possible applications of these glasses for emission in the near- or mid-infrared spectral region.

Acknowledgement

The work was supported by grant No. 203/98/0103 of Czech Grant Agency, by grant No. 2383/1999 of the University of Pardubice and by the "Key project 12/96" of Czech Acad. Sci., Prague, which are gratefully acknowledged. We are grateful to Dr Chvostová, Institute of Physics, Czech Academy of Sciences, Prague, for ellipsometric determination of the indices of refraction.

References

[1] Brocklesby W. S, Pearson A., J. Lumin. **59**, 333(1994).
[2] Frumarová B., Oswald J., Krečmer P., Frumar M., Černý V., Smrčka V., Opt. Mater. **6**, 217(1996).
[3] Frumarová B., Němec P., Frumar M., Oswald J., Vlček M., J. Non-Cryst. Solids **256-257**, 266 (1999).
[4] Schweizer T., Hewak D.W., Samson B.N., Payne D.N., Opt. Lett. **21,** 1594(1996).
[5] Wei K., Machewirth D.P., Wenzel J., Snitzer, E., Sigel G.H. Jr., Opt. Lett. **19,** 904(1994).
[6] Nachimuthu P., Jagannathan R., Nirmal V., Kumar, D. Narayana Rao, J. Non-Cryst. Solids **217**, 215(1997).
[7] Binnemans K., Van Deun R., Goerller-Walrand C., Adam J.L., J. Non-Cryst. Solids **238**, 11(1998).
[8] Mahato K. K., Rai D.K., Rai S.B., Solid State Com. **108,** 671(1998).
[9] Farries M.C., Morkel P.R., Townsend J.E., IEE Proceedings **137,** 318(1990).
[10] Němec P., Frumarová B., Frumar M., J. Non-Cryst. Solids (1999), in press.
[11] Adam J.L., Docq A.D., Lucas J., J. Solid State Chem. **75**, 403(1988).
[12] Judd J. B. R., Phys. Rev. **127**, 750(1962).
[13] Ofelt G. S., J. Chem. Phys. **37**, 511(1962).
[14] Carnall W.T., Crosswhite H., Crosswhite H.M., Argonne National Laboratory Report ANL-78-XX-95, 1978.
[15] Adam J.L., Guimond Y., Jurdyc A.M., Griscom L., Mugnier J., Jacquier B., SPIE **3280**, 31(1998).